Pattern engineering of living bacterial colonies using meniscus-driven fluidic channels

Vasily Kantsler[1,2,*], Elena Ontañón-McDonald[3,#], Cansu Kuey[3,#], Manjari J Ghanshyam[3], Maria Chiara Roffin[1] and Munehiro Asally[3,4,*]

[1] Department of Physics, University of Warwick, Coventry, CV4 7AL, United Kingdom
[2] Warwick Medical School, University of Warwick, Coventry, CV4 7AL, United Kingdom
[3] School of Life Sciences, University of Warwick, Coventry, CV4 7AL, United Kingdom
[4] Warwick Integrative Synthetic Biology Centre, University of Warwick, Coventry, CV4 7AL, United Kingdom
[#] Equal contribution
[*] Correspondence should be addressed to VK (v.kantsler@warwick.ac.uk) or MA (m.asally@warwick.ac.uk)

ORCID:

VK 0000-0002-1895-7754
MA 0000-0002-8273-7617

Abstract

Creating adaptive, sustainable and dynamic biomaterials is a forthcoming mission of synthetic biology. Engineering spatially organized bacterial communities has a potential to develop such bio-metamaterials. However, generating living patterns with precision, robustness and low-technical barrier remains as a challenge. Here we present an easily implementable technique for patterning live bacterial populations using a controlled meniscus-driven fluidics system, named as MeniFluidics. We demonstrate multiscale patterning of biofilm colonies and swarms with submillimeter resolution. Utilizing the faster bacterial spreading in liquid channels, MeniFluidics allows controlled bacterial colonies both in space and time to organize fluorescently labelled *Bacillus subtilis* strains into a converged pattern and to form dynamic vortex patterns in confined bacterial swarms. The robustness, accuracy and low technical barrier of MeniFluidics offer a tool for advancing and inventing new living materials that can be combined with genetically engineered systems, and adding to fundamental research into ecological, evolutional and physical interactions between microbes.

Keywords

Cell Biophysics; Soft Matter; Living materials; Swarming; Biofilms; Pattern Engineering

Owing to their multifunctional nature, bacterial communities represent sources of inspirations and opportunities for scientists and engineers to create adaptive and programmable engineered living materials (ELM) [1–3]. Self-organized bacterial communities, such as biofilms and swarms, exhibit complex multicellular behaviors which promote the survival of cells in harsh environments [4–7]. Through metabolic and biophysical cell-cell interactions, biofilms also produce valuable chemicals and materials that can be used for next-generation batteries, biofuels, biodegradable plastics or therapeutics [8,9]. Arrangements of microbes in space and time are crucial for these collective behaviors and functions, and hence controlling bacterial communities in space and time is an important step towards creating living functional materials [10,11]. ELM has a potential to go beyond the traditional understanding of materials as a static set of properties by having adaptive and dynamic properties. Intriguingly, recent progresses in theoretical understanding of topological active matter (e.g. [12–14]) raise an exciting possibility of manufacturing programmable, adaptive and fluidic metamaterials [15]. However, implementing these theoretical designs is yet to be seen because it requires advances in experimental techniques for controlling active constituents and their collectives on multiple scales.

Substantial amount of bioengineering effort in the last decade has been exploited for developing living cells and biomaterials that self-organize into desired patterns [3,16]. For example, programable nano-objects and biomaterials were developed by functionalizing amyloid fibril [17,18], the main protein component of biofilm matrix [19,20]. Bacterial populations can be organized into patterns using inkjet printers [21], microcontact printing [22], 3D printing [23,24], biofilm lithography [25] or genetic engineering [26–28]. Yet, controlling the emergent dynamic patterns, such as vortices, remains largely unexplored. Furthermore, their associated high technical and expertise barriers, demanding precise control of tools, customized equipment and/or extensive genetic modifications, hinder the wide use of these techniques. A robust and easy method to precisely control microbial patterns in space and time is essential to unleash the full potential of biofilm engineering and facilitate biomaterial innovations.

Here we present MeniFluidics, a technique for micro-patterning fluid meniscus layers. We demonstrate that local acceleration of bacterial spreading via MeniFluidics can shape biofilms into desired static and active patterns, arrange multiple stains into controlled proximity and provide a tool to study self-organization dynamics of active fluids in confinement.

RESULTS

Rationalized gel surface structuring for micropatterned channel formation

The idea of MeniFluidics stems from the notion that a structured agar gel with a sharp concave edge can be wetted by a fluid meniscus layer (Fig. 1, S1 and S2). This fluidics layer could provide a favorable path for cells to spread in space, which would in turn enable us to control the directions of colony growth. To implement this idea, we made a structured agar surface by placing a micropatterned PDMS mold on an agar plate during solidification (Fig. 1b, c, *see also* Fig. S3 and S4). Microscopy imaging of the structure shows the meniscus radius of curvature with a few tens of microns (*see* Fig. S1). This length is much smaller than the water capillary length, defined by the balance of the fluid surface tension to the gravity force: $L_c = \sqrt{\sigma/\rho g}$, where σ and ρ are the surface tension and the density of the fluid, respectively. This small meniscus radius could be attributed to the reduced water pressure in agar ($P_{agar} < P_{atm}$) due to elastic contraction of agar gel. After gelation, the elastic matrix of agar contracts due to evaporation of the water phase, which creates an extensile force acting on the fluid that gives

rise to a reduced pressure in the agar. When we assume a linear response of the elastic agar gel, the pressure P_{agar} can be estimated as $P_{atm} - E\Delta$, where $\Delta = \delta/A$ is a ratio of the evaporated volume of water (δ) from the agar to the total volume of agar layer (A) after gelation and E is the Young's elastic modulus of the agar gel. The meniscus radii, R, can be estimated by the Young-Laplace equation:

$$E\Delta = \sigma\left(\frac{1}{R_1} + \frac{1}{R_2}\right) \quad (1)$$

where R_1 and R_2 are principal radii of the curvature. In the case of a plane meniscus with a linearly structured agar (Fig. 1a-c, S1a and b), $1/R_2$ is negligible and we have $R_1 = \frac{\sigma}{E}\Delta^{-1}$. Measured variation of R_1 as a function of Δ for 1.5% agar gel in water reveals that the decay is slightly slower than Δ^{-1} (Fig. S1). This indicates that agar does not act as an ideal Hookean spring, but possibly exhibits plastic deformations. The measurements estimates the Young modulus of the agar to be $\sim 10^4 - 10^5 Pa$, which is in agreement with reported values [29]. Importantly, the meniscus width behaves as a function of Δ, and hence it can be maintained for days when keeping the relative humidity high (Fig. S1). Accounting for the fact that a complex medium reduces the surface tension in comparison to water [30], we obtain the meniscus radius of curvature R_1 to be in the order of a few tens of microns, which is again in good agreement with the observation. Altogether, our analysis and optical observation clearly indicate that structured agar surface can create fluidic channels with a cross section size $h = R_1\left(1 - \sin\frac{\pi}{4}\right) \approx 0.3R_1$ due to the pressure difference between inside and outside of agar.

Controlled biofilm spreading by MeniFluidics over Space

To verify if the formed meniscus layers are large enough to contain bacterial cells, we began by inoculating *B. subtilis* cells onto a structured agar surface and observed them under a microscope. Bacterial cells were visible in the regions within ~16 μm from the edge of the micro-patterned structures and moving along the structure in real time (Fig. 1d, Fig. S5 and Supporting Movie S1). This observation confirms that the meniscus is sufficiently large to carry bacterial cells. We next examined whether the meniscus channels enable controlling the directions of macroscopic bacterial colony spreading. Inoculum of a biofilm-forming *B. subtilis* strain, NCIB3610, was placed on flat agar surface approximately 3 mm away from a micro-patterned structure (Fig. 1e). The plate was incubated at 30°C and imaged using a custom-built DSLR camera imaging setup (see Methods). The colony initially grew isotropically on a flat agar surface and eventually stopped after expanding for ~2.5 cm, as previously reported [31]. When the expanding edge reached the MeniFluidics channel, the edge locally expanded rapidly with the measured speed of ~10 mm/hr (Fig. 1f, g, and Supporting Movie S2). While this speed may be influenced by both the cell spreading through the channel and the following lateral growth, it is evident that the MeniFluidic channel substantially accelerates the colony expansion. To confirm that the MeniFluidics-guided expansion is not specific to *B. subtilis*, we repeated the experiment with *E. coli*, the Gram-negative model bacterium and confirmed a rapid expansion through the channel with *E. coli* (Fig. S6). These results provide a proof of concept that MeniFluidics can be used to control the directions of bacterial growth on gel surfaces.

Controlled biofilm spreading by MeniFluidics over Time

The gained spatial control over biofilm expansion holds a question of whether the overall expansion speed can also be tuned. To this end, we consider a geometrically imposed control over the meniscus radii by introducing a convex structure which creates the second principle radius of curvature, R_2 (Fig. S2). Introduction of the second principal radius of curvature R_2 may alter R_1, thus the channel size, as denoted by the Young-Laplace equation (Eq. 1). Specifically, when $E\Delta$ and σ are constant, a small negative convex R_2 decreases R_1, while small positive concave R_2 increases R_1. This means that when

R_1 becomes too small to carry bacterial cells, the translocation of cells along MeniFluidic channels should cease off. According to this picture, we speculated that a highly curved structure supporting the meniscus should introduce breaks in MeniFluidics where the expansion dramatically slows down.

To test the conjecture, we introduced an additional structure with a sharp 90° curve, named as "hinges", which would break the bacterial flow at their high curvature tips (Fig. 2a). We created channels with periodically spaced hinges with a period of 4 mm ($D_g = 4\ mm$), and inoculated bacteria onto the flat agar surface a few millimeters away from the channel. The expansion speeds were measured at 30°C using a DSLR camera imaging setup. The colony exhibited a regular oscillation of fast and slow expansion phases in its growth along the channel (Fig. 2b, c, and Supporting Movie S3). The distances between halts were in good agreement with D_g, indicating slowed expansion by the hinges (Fig. 2b). To demonstrate that hinges allow controlling the overall expansion speeds, we repeated the experiment with the designs with various distances between hinges (D_g). The result shows that the overall expansion speed increases as a function of D_g (Fig. 3d). When the colony is assumed to follow the meniscus at maximum velocity V_m over distance D_g and delay at a hinge for a time τ, the average velocity V of the colony edge along the hinged MeniFluidics is:

$$V = \frac{D_g}{\frac{D_g}{V_m} + \tau} \quad (2)$$

Estimating $V_m \approx 10\ mm/hr$ and $\tau \approx 8\ hr$ from the obtained data, we can see that the Eq.2 fits the data well (Fig. 3d), indicating that hinged MeniFluidics allow controlling the colony expansion speed in a predictive manner.

Pattern engineering of biofilms and swarming dynamics

We next wondered if the gained ability may allow us to create bacterial colonies into arbitrary designed patterns. As a proof of concept, we designed and implemented a snow-flake-like and a flower-like patterned MeniFluidics channels and inoculated bacteria to the centers of the designs. After ~2 days of incubation at 30°C, biofilms were formed with the designed shapes (Fig. 3a, b, S8 and Supporting Movie S4). To further demonstrate the versatility of MeniFluidics, we designed an interdigitated pattern in which two bacterial strains can form a stripe pattern in the middle (Fig. 3c). For visualization of different strains, we used fluorescently labelled bacterial strains and inoculated them at the other ends of the pattern. Specifically, we inoculated yellow fluorescent protein (YFP) or cyan fluorescent protein (CFP) expressing *B. subtilis*, but otherwise identical, strains and incubated at 30°C for 2 days. The YFP-labelled and CFP-labelled strains were organized into the designed pattern and formed an alternating pattern in the middle where the distance between two strains can be robustly controlled (Fig. 3d, e). Notably, MeniFluidics does not require any special equipment or use of genetically modified strains. Even if microfabricated molds are not readily available, the method can be applied because meniscus layers, and thus MeniFluidics, can be formed by any boundary of an object placed on an agar surface. As an example, we placed a metal piece on agar surface and inoculated *B. subtilis* cells a few millimeters away from the object. As expected, bacterial colony expansion was accelerated around the metal piece, resulting in a metal piece surrounded by a wrinkled biofilm colony (Supporting Movie S6).

Finally, we tested if MeniFluidics can be adapted for forming dynamic patterns of active matter, such as motile bacterial cells. We implemented MeniFluidics to confine actively swarming *B. subtilis* cells in micron-sized domains consisting of circular, elliptical, and rectangular wells. The structured domains were populated by swarming bacteria, which facilitated bacterial turbulence phenomenon under confinement (Fig. 4a-d and Supporting Movie S5). Swarming bacteria entrained microscopic wells,

while the gel parameters (i.e. E and Δ) were tuned in such a way that the meniscus radii of curvature considerately exceed the width of the wells. This resulted in a fluid layer within the compartments, where bacterial active motion was facilitated. The results revealed an interesting case of spiral vortices, vortex lattices and bacterial turbulence which are reminiscent of what have been reported in microfluidic confinement and isolated droplets [32–34]. These results thus demonstrate that MeniFluidics can indeed be used for forming dynamic patterns of active matter.

DISCUSSION

This study presents a new method for controlling the spatial distributions of microbes, which has implications for fundamental research into synthetic biology, bioengineering, biophysics, microbiology and ecology and developments of novel fluidic metamaterials. We show that the method can be used with phylogenetically different bacterial species, namely *B. subtilis* and *E. coli,* and for arbitrary designed patterns (Fig. 1 - 3). A notable feature of MeniFluidics is that it allows formation of dynamic turbulence patterns (Fig. 4), which could open a new avenue for the research into active matter and fluidic metamaterial developments. For these assays, MeniFluidics extends the lifetime of collective dynamics in the system for several hours due to bacteria's unrestricted access to oxygen. This is in contrast to the bacterial collective dynamics in microfluidics, where motility only lasts ~10 minutes because of oxygen depletion [35,36]. MeniFluidics also enables controlling the colony growth both in space and time, which has not been achieved by previously reported technologies (e.g. [22–24]). It is also worth noting that, unlike the other methods that typically require customized special equipment or extensive genetic modifications, MeniFluidics does not require any special equipment and thus allows broad use of the method. We demonstrated that placing an object on agar surface is sufficient in forming MeniFluidics (Supporting Movie S6). While we used PDMS for patterning agar surfaces, micro-patterned materials can be also produced by other methods, such as cutter plotters, 3D printers or micro-machining.

Among many exciting applications of the methods is developing living materials for bioremediation via spatial control of microbial communities. For example, MeniFluidics could be designed to spatially organize multiply engineered strains to facilitate the biodegradation of toxic compounds requires spatial organization of multiple engineered strains [37]. The interdigitated pattern presented in this work could be useful for studying the impacts of spatial distances to microbial interactions for engineering microbial communities. It can also be used to induce autoinhibition of bacterial populations via sibling competition mechanism [38]. Another application could be using the fast boundary propagation of bacteria along the MeniFluidic pattern for an assessment of collective antimicrobial tolerance. Agar plates with a spatial gradient of antimicrobial compounds can be modified by parallel ridges structure, while asymmetry in propagation of the colony along the menisci can indicate antimicrobial response. Furthermore, the proof of principle of the method may be extended for tissue engineering with mammalian cells because mammalian cells can only thrive in liquid, such as in MeniFluidic channels.

Our observation is in an interesting conjunction with the phenomenon known as "fungal highways" where fungi hypae and mycelium promote the dispersal of bacteria on cheese, potatoes and various surfaces [39,40]. While the exact physical mechanism behind the fungal highways is unknown, our study suggests that fungal hypae may create natural MeniFluidics in which bacteria spreading is accelerated. Fungal highways have been observed with various species of fungi and bacteria, which supports the idea that physics underlines this cross-kingdom interaction. MeniFluidics could allow dissecting the biochemical interactions from physical interactions between fungi and bacteria through controlled

experimentation of multispecies microbiota. Therefore, this method is not only useful for engineering living materials but also to advance experimental research in microbial biophysics and ecology.

METHODS

Strains and growth conditions

B. subtilis and *E. coli* cells were routinely grown in Lysogeny Broth (LB) or on LB agar plate (agar 1.5% (w/v), agar 1% (w/v) for swarming experiments). The strains used in this study are listed in Table 1. For MeniFluidics experiments, a single colony from LB agar plate was inoculated into LB and cultured for ~6 hours at 37°C with aeration (200 rpm). Cells were then inoculated onto minimal salts glutamate glycerol (MSgg) media [4]: 5 mM potassium phosphate (pH 7.0), 100 mM morpholine propane sulfonic acid (MOPS) (pH 7.0), 2 mM MgCl2, 700 µM CaCl2, 50 µM MnCl2, 100 µM FeCl3, 1 µM ZnCl2, 2 µM thiamine-HCl, 0.5% (v/v) glycerol, 0.5% (w/v) monosodium glutamate and 1.5% (w/v) agar. For swarming experiments, 5 µl of the culture was inoculated on 1% (w/v) agar plate 8 hours prior to the swarming measurements.

PDMS stamps and patterning agar surfaces

Patterns for MeniFluidics were fabricated on four-inch silicon wafers using a conventional soft lithography technique [41]. The master mold was produced from SU8 2035 (MicroChem), spun to a 50-µm-thick layer, and exposed to UV light through a high-resolution mask (Micro lithography services) to obtain the desired structures. Polydimethylsiloxane (PDMS) (Sygard 184, Dow Corning Corp) prepolymer was mixed at a ratio of 10:1 (w/w) with curing agent and poured on top of silicon wafer mold. After degassing the mixture, PDMS was cured at 100°C for 1 hour. The cured PDMS was peeled off from Silicon wafer mold for stamping patterns on agar plates. To transfer the features onto agar plates, MSgg or LB media were poured into plastic dishes (40 mL to 150 mm plates, 20 mL to 90 mm plates) and set to solidify for 30-60 min (*see* Fig. S3). Solidified plates were warmed on a 70°C plate while 10 ml (for 150 mm petri dish) and 5 ml (for 90 mm petri dish) media were poured as a second layer. Autoclaved PDMS with features, pre-warmed at 50°C, were gently placed on the second layer. Bubbles were removed by tapping with the end of the forceps. After solidification of the second layers, PDMS was removed. Plates were dried at 37°C overnight.

Time-lapse imaging

Biofilms formation was recorded using a digital single-lens reflex camera (DSLR, Nikon D5300) in a 30°C incubator. AF-S DX Micro NIKKOR 40mm f/2.8G macro lens and AF-P DX NIKKOR 10-20mm f/4.5-5.6G VR ultra-wide zoom lens were used. A custom-built imaging platform was assembled to place the camera perpendicular to plates (Fig. S4). The items used for the assembly of the platform are listed in Table 2. Images were taken every hour using the built-in internal time shooting function of D5300. For microscopy, images were obtained by an inverted fluorescence microscope (Leica, DMi8) with HC PL FLUOTAR 40x/0.60 Ph2.

Video-microscopy of swarming and menisci radii

The swarming under confinement and the measurements of the menisci radii was recorder by inverted microscope Nikon TE2000U with 20x/0.45 Ph1 lens at 50fps using Point Grey GS3-U3-23S6M-C camera (FLIR). The velocity fields from the image sequences were obtained via open source MatPIV toolbox (version 1.61). The menisci radii measurements were undertaken with 160 microns structure on 1.5% agar gel in deionized water. The agar plate has been weighted immediately after gel molding.

The relative reduced mass of the gel, Δ, has been obtained through the mass measurements with a precision in Δ of 0.6×10^{-3}. The image was aligned with the inner corner of the structure, then the focus had been moved to the tip of the meniscus. The intensity profile has been averaged along the image symmetry (y-axis) and the tip position has been identified manually with an uncertainty of 0.9 microns (see Fig. S1).

SUPPORTING INFORMATION

Figures S1 and S2, Characterization of meniscus; S3, Illustrated procedure; S4, Imaging setup; S5, Single-cell images of bacteria in MeniFluidics; S6, *E. coli* colony expansion by MeniFluidics; S7, *B. subtilis* colony expansion by MeniFluidics with hinges; S8, Time series of *B. subtilis* pattern formation; Table S1, Bacterial strains used in this study; Table S2, List of items for imaging stand; Supplementary Movies corresponding to Figures.

ACKNOWLEDGEMENTS

We acknowledge Yuandi Wei and Dario Bazzoli for their experimental attempts with MeniFluidics. We thank Drs. Marco Polin, Orkun Soyer, Jorn Dunkel and Dong-yeon Lee for their critical comments to early versions of the manuscript. We also thank Drs. Petr Denissenko and Gareth Alexander for helpful discussions. VK gratefully acknowledges support from British Council Link Travel Grant (2017-RLTG8-10229) and welcoming hosting of Dr. Avraham Beer in his lab at Jacob Blaustein Institute for Desert Research, Israel. This project was financially supported by University of Warwick School of Life Sciences pump prime funding and BBSRC/EPSRC Synthetic Biology Centre grant (BB/M017982/1) to MA and EPSRC/BBSRC Synthetic Biology Centre for Doctoral Training grant (EP/L016494/1) to CK.

AUTHOR CONTRIBUTIONS

VK and MA conceived the project and designed experiments. VK analyzed the theory of meniscus formation. EOM, CK and VK performed experiments. EOM designed bio-art patterns. VK, MJG and MCR prepared materials for experiments. VK, MA and CK analyzed data. MA and VK supervised the project. MA and VK wrote the manuscript with the inputs from other authors.

CONFLICT OF INTEREST

The authors declare no conflict of interest.

REFERENCES

(1) Nguyen, P. Q. Synthetic Biology Engineering of Biofilms as Nanomaterials Factories. *Biochem. Soc. Trans.* **2017**, *45* (3), 585–597. https://doi.org/10.1042/bst20160348.

(2) Brenner, K.; You, L.; Arnold, F. H. Engineering Microbial Consortia: A New Frontier in Synthetic Biology. *Trends Biotechnol.* **2008**, *26* (9), 483–489. https://doi.org/10.1016/j.tibtech.2008.05.004.

(3) Chen, A. Y.; Zhong, C.; Lu, T. K. Engineering Living Functional Materials. *ACS Synth. Biol.* **2015**, *4* (1), 8–11. https://doi.org/10.1021/sb500113b.

(4) Asally, M.; Kittisopikul, M.; Rue, P.; Du, Y.; Hu, Z.; Cagatay, T.; Robinson, A. B. A. B.; Lu, H.; Garcia-Ojalvo, J.; Suel, G. M.; et al. Localized Cell Death Focuses Mechanical Forces during 3D Patterning in a Biofilm. *Proc. Natl. Acad. Sci.* **2012**, *109* (46), 18891–18896. https://doi.org/10.1073/pnas.1212429109.

(5) Nadell, C. D.; Drescher, K.; Foster, K. R. Spatial Structure, Cooperation and Competition in Biofilms. *Nat. Rev. Microbiol.* **2016**, *14* (9), 589–600. https://doi.org/10.1038/nrmicro.2016.84.

(6) Wilking, J. N.; Angelini, T. E.; Seminara, A.; Brenner, M. P.; Weitz, D. a. Biofilms as Complex Fluids. *MRS Bull.* **2011**, *36* (05), 385–391. https://doi.org/10.1557/mrs.2011.71.

(7) Liu, J.; Prindle, A.; Humphries, J.; Gabalda-Sagarra, M.; Asally, M.; Lee, D.; Ly, S.; Garcia-Ojalvo, J.; Süel, G. M. Metabolic Co-Dependence Gives Rise to Collective Oscillations within Biofilms. *Nature* **2015**, *523* (7562), 550–554. https://doi.org/10.1038/nature14660.

(8) Wood, T. K.; Hong, S. H.; Ma, Q. Engineering Biofilm Formation and Dispersal. *Trends Biotechnol.* **2011**, *29* (2), 87–94. https://doi.org/10.1016/j.tibtech.2010.11.001.

(9) Douglas, S. Mineral Formation by Bacteria in Natural Microbial Communities. *FEMS Microbiol. Ecol.* **2002**, *26* (2), 79–88. https://doi.org/10.1016/s0168-6496(98)00027-0.

(10) Jiang, X.; Zerfaß, C.; Feng, S.; Eichmann, R.; Asally, M.; Schäfer, P.; Soyer, O. S. Impact of Spatial Organization on a Novel Auxotrophic Interaction among Soil Microbes. *ISME J.* **2018**, *12* (6), 1443–1456. https://doi.org/10.1038/s41396-018-0095-z.

(11) Nagy, K.; Ábrahám, Á.; Keymer, J. E.; Galajda, P. Application of Microfluidics in Experimental Ecology: The Importance of Being Spatial. *Front. Microbiol.* **2018**, *9*, 496. https://doi.org/10.3389/fmicb.2018.00496.

(12) Dasbiswas, K.; Mandadapu, K. K.; Vaikuntanathan, S. Topological Localization in Out-of-Equilibrium Dissipative Systems. *Proc. Natl. Acad. Sci.* **2018**, *115* (39), E9031–E9040. https://doi.org/10.1073/pnas.1721096115.

(13) Souslov, A.; Van Zuiden, B. C.; Bartolo, D.; Vitelli, V. Topological Sound in Active-Liquid Metamaterials. *Nat. Phys.* **2017**, *13* (11), 1091–1094. https://doi.org/10.1038/nphys4193.

(14) Woodhouse, F. G.; Dunkel, J. Active Matter Logic for Autonomous Microfluidics. *Nat. Commun.* **2017**, *8*, 1–7. https://doi.org/10.1038/ncomms15169.

(15) Alù, A. Prime Time. *Nat. Mater.* **2016**, *15* (12), 1229–1231. https://doi.org/10.1038/nmat4814.

(16) Gilbert, C.; Ellis, T. Biological Engineered Living Materials: Growing Functional Materials with Genetically Programmable Properties. *ACS Synth. Biol.* **2018**, *8*, 1–15. https://doi.org/10.1021/acssynbio.8b00423.

(17) Nguyen, P. Q.; Botyanszki, Z.; Tay, P. K. R.; Joshi, N. S. Programmable Biofilm-Based Materials from Engineered Curli Nanofibres. *Nat. Commun.* **2014**, *5*, 1–10. https://doi.org/10.1038/ncomms5945.

(18) Chen, A. Y.; Deng, Z.; Billings, A. N.; Seker, U. O. S.; Lu, M. Y.; Citorik, R. J.; Zakeri, B.; Lu, T. K. Synthesis and Patterning of Tunable Multiscale Materials with Engineered Cells. *Nat. Mater.* **2014**, *13* (5), 515–523. https://doi.org/10.1038/nmat3912.

(19) DePas, W. H.; Chapman, M. R. Microbial Manipulation of the Amyloid Fold. *Res. Microbiol.* **2012**, *163* (9–10), 592–606. https://doi.org/10.1016/j.resmic.2012.10.009.

(20) Taglialegna, A.; Lasa, I.; Valle, J. Amyloid Structures as Biofilm Matrix Scaffolds. *J. Bacteriol.* **2016**, *198* (19), 2579–2588. https://doi.org/10.1128/JB.00122-16.

(21) Merrin, J.; Leibler, S.; Chuang, J. S. Printing Multistrain Bacterial Patterns with a Piezoelectric Inkjet Printer. *PLoS One* **2007**, *2* (7). https://doi.org/10.1371/journal.pone.0000663.

(22) Weibel, D. B.; Lee, A.; Mayer, M.; Brady, S. F.; Bruzewicz, D.; Yang, J.; Diluzio, W. R.; Clardy, J.; Whitesides, G. M. Bacterial Printing Press That Regenerates Its Ink: Contact-Printing Bacteria Using Hydrogel Stamps. *Langmuir* **2005**, *21* (14), 6436–6442. https://doi.org/10.1021/la047173c.

(23) Connell, J. L.; Ritschdorff, E. T.; Whiteley, M.; Shear, J. B. 3D Printing of Microscopic Bacterial Communities. *Proc. Natl. Acad. Sci.* **2013**, *110* (46), 18380–18385. https://doi.org/10.1073/pnas.1309729110.

(24) Schaffner, M.; Rühs, P. A.; Coulter, F.; Kilcher, S.; Studart, A. R. 3D Printing of Bacteria into Functional Complex Materials. *Sci. Adv.* **2017**, *3* (12). https://doi.org/10.1126/sciadv.aao6804.

(25) Jin, X.; Riedel-Kruse, I. H. Biofilm Lithography Enables High-Resolution Cell Patterning via Optogenetic Adhesin Expression. *Proc. Natl. Acad. Sci.* **2018**, *115* (14), 3698–3703. https://doi.org/10.1073/pnas.1720676115.

(26) Karig, D.; Martini, K. M.; Lu, T.; DeLateur, N. A.; Goldenfeld, N.; Weiss, R. Stochastic Turing Patterns in a Synthetic Bacterial Population. *Proc. Natl. Acad. Sci.* **2018**, *115* (26), 6572–6577. https://doi.org/10.1073/pnas.1720770115.

(27) Liao, M. J.; Din, M. O.; Tsimring, L.; Hasty, J. Rock-Paper-Scissors: Engineered Population Dynamics Increase Genetic Stability. *Science* **2019**, *365* (6457), 1045–1049. https://doi.org/10.1126/science.aaw0542.

(28) Kan, A.; Del Valle, I.; Rudge, T.; Federici, F.; Haseloff, J. Intercellular Adhesion Promotes Clonal Mixing in Growing Bacterial Populations. *J. R. Soc. Interface* **2018**, *15* (146). https://doi.org/10.1098/rsif.2018.0406.

(29) Nayar, V. T.; Weiland, J. D.; Nelson, C. S.; Hodge, A. M. Elastic and Viscoelastic Characterization of Agar. *J. Mech. Behav. Biomed. Mater.* **2012**, *7*, 60–68. https://doi.org/10.1016/j.jmbbm.2011.05.027.

(30) Rühs, P. A.; Böni, L.; Fuller, G. G.; Inglis, R. F.; Fischer, P. In-Situ Quantification of the Interfacial Rheological Response of Bacterial Biofilms to Environmental Stimuli. *PLoS One* **2013**, *8* (11). https://doi.org/10.1371/journal.pone.0078524.

(31) Seminara, A.; Angelini, T. E.; Wilking, J. N.; Vlamakis, H.; Ebrahim, S.; Kolter, R.; Weitz, D. A.; Brenner, M. P. Osmotic Spreading of Bacillus Subtilis Biofilms Driven by an Extracellular Matrix. *Proc. Natl. Acad. Sci.* **2012**, *109* (4), 1116–1121. https://doi.org/10.1073/pnas.1109261108.

(32) Wioland, H.; Lushi, E.; Goldstein, R. E. Directed Collective Motion of Bacteria under Channel Confinement. *New J. Phys.* **2016**, *18* (7). https://doi.org/10.1088/1367-2630/18/7/075002.

(33) Lushi, E.; Wioland, H.; Goldstein, R. E. Fluid Flows Created by Swimming Bacteria Drive Self-Organization in Confined Suspensions. *Proc. Natl. Acad. Sci.* **2014**, *111* (27), 9733–9738. https://doi.org/10.1073/pnas.1405698111.

(34) Doostmohammadi, A.; Shendruk, T. N.; Thijssen, K.; Yeomans, J. M. Onset of Meso-Scale Turbulence in Active Nematics. *Nat. Commun.* **2017**, *8*, 1–7. https://doi.org/10.1038/ncomms15326.

(35) Tuval, I.; Cisneros, L.; Dombrowski, C.; Wolgemuth, C. W.; Kessler, J. O.; Goldstein, R. E. Bacterial Swimming and Oxygen Transport near Contact Lines. *Proc. Natl. Acad. Sci.* **2005**, *102* (7), 2277–2282. https://doi.org/10.1073/pnas.0406724102.

(36) Dunkel, J.; Heidenreich, S.; Drescher, K.; Wensink, H. H.; Bär, M.; Goldstein, R. E. Fluid Dynamics of Bacterial Turbulence. *Phys. Rev. Lett.* **2013**, *110* (22), 228102. https://doi.org/10.1103/PhysRevLett.110.228102.

(37) de Lorenzo, V. Synthetic Microbiology: From Analogy to Methodology. *Microb. Biotechnol.* **2017**, *10* (5), 2–4. https://doi.org/10.1111/1751-7915.12786.

(38) Be'er, A.; Ariel, G.; Kalisman, O.; Helman, Y.; Sirota-Madi, A.; Zhang, H. P.; Florin, E.-L. E.-L.; Payne, S. M.; Ben-Jacob, E.; Swinney, H. L. Lethal Protein Produced in Response to Competition between Sibling Bacterial Colonies. *Proc. Natl. Acad. Sci.* **2010**, *107* (14), 6258–

6263. https://doi.org/10.1073/pnas.1001062107.

(39) Kohlmeier, S.; Smits, T. H. M.; Ford, R. M.; Keel, C.; Harms, H.; Wick, L. Y. Taking the Fungal Highway: Mobilization of Pollutant-Degrading Bacteria by Fungi. *Environ. Sci. Technol.* **2005**, *39* (12), 4640–4646. https://doi.org/10.1021/es047979z.

(40) Zhang, Y.; Kastman, E. K.; Guasto, J. S.; Wolfe, B. E. Fungal Networks Shape Dynamics of Bacterial Dispersal and Community Assembly in Cheese Rind Microbiomes. *Nat. Commun.* **2018**, *9* (1), 1–12. https://doi.org/10.1038/s41467-017-02522-z.

(41) Xia, Y.; Whitesides, G. M. Soft Lithography. *Annu. Rev. Mater. Sci.* **1998**, *28* (1), 153–184. https://doi.org/10.1146/annurev.matsci.28.1.153.

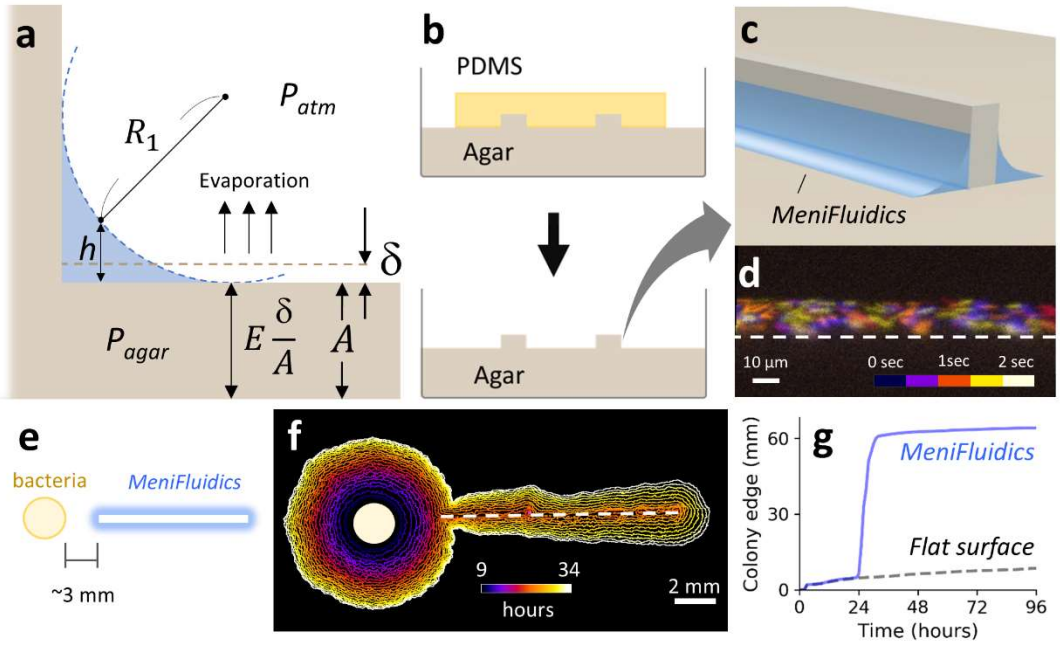

Figure 1. a) Schematic illustration of meniscus layer (blue) formed on structured agar surface (beige). When $1/R_2 \sim 0$, $R_1 = \sigma/E\Delta$ as denoted by the Young-Laplace equation (Eq.1), $h = R_1(1 - sin\frac{\pi}{4}) \approx 0.3R_1$, E is Young's modulus, δ is the volume loss due to evaporation, A is the volume of agar, σ is surface tension, and P is the pressure. b, c) Schematics of the MeniFluidics formation through PDMS molding on agar. d) Projected time-lapse microscopy image of meniscus channel populated by bacteria. Colours denote time points of observation in seconds. Dashed line indicates the edge of structure (see Figure S3 and Supporting Movie S1 for corresponding brightfield image). e) Schematic illustration of experiment where bacteria were inoculated ~3 mm away from MeniFluidics. f) Representative time evolution of a *B. subtilis* biofilm grown on agar with MeniFluidics. g) Distances of the biofilm colony edge from the centre on flat agar surface (dashed grey) and MeniFluidics channel (blue).

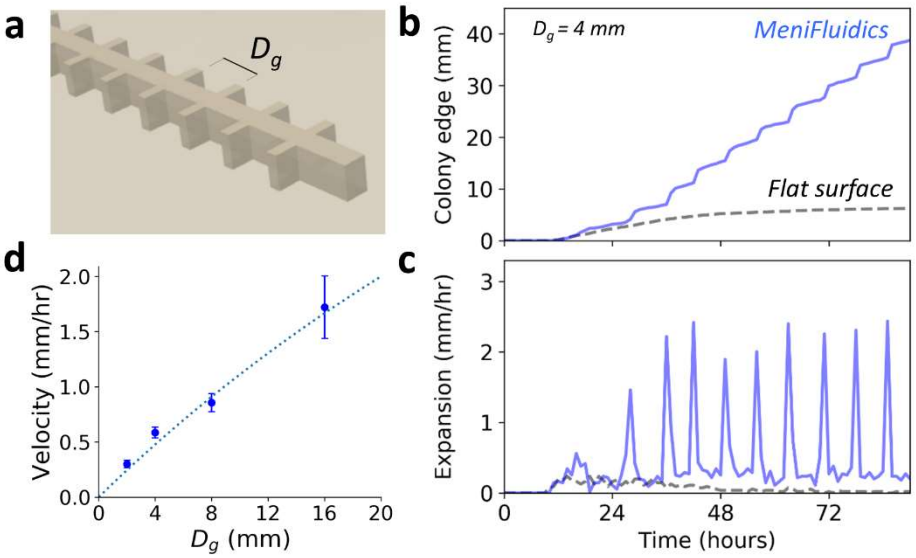

Figure 2. a) Schematic illustration of 3D structure with hinges. D_g is the distance between hinges. b) Representative graphs of *B. subtilis* colony edge and c) expansion speed over time along hinged MeniFluidics with $D_g = 4\ mm$. d) Mean overall expansion speed as a function of D_g. Dashed line is Eq. 2 with $V_m = 10\ mm/hr, \tau = 8\ hr$. Error bars are standard deviations.

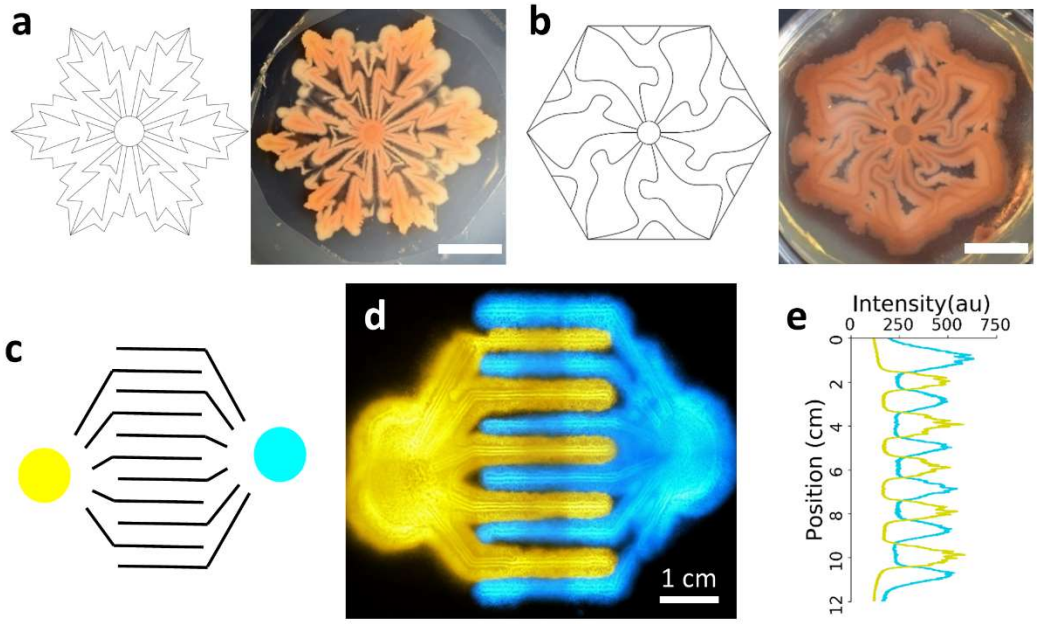

Figure 3. a, b) Arbitrary designed MeniFluidics patterns (left) and patterned *B. subtilis* biofilms formed by the corresponding designs (right). Scale bar, 2 cm. c) Schematic of interdigitated MeniFluidic design. Yellow and cyan circles are inoculation points of fluorescently labelled bacterial strains. d) Representative fluorescence microscopy image of biofilms formed by YFP (yellow) or CFP (cyan) expressing bacteria. e) Fluorescence intensity across the dashed line in panel d.

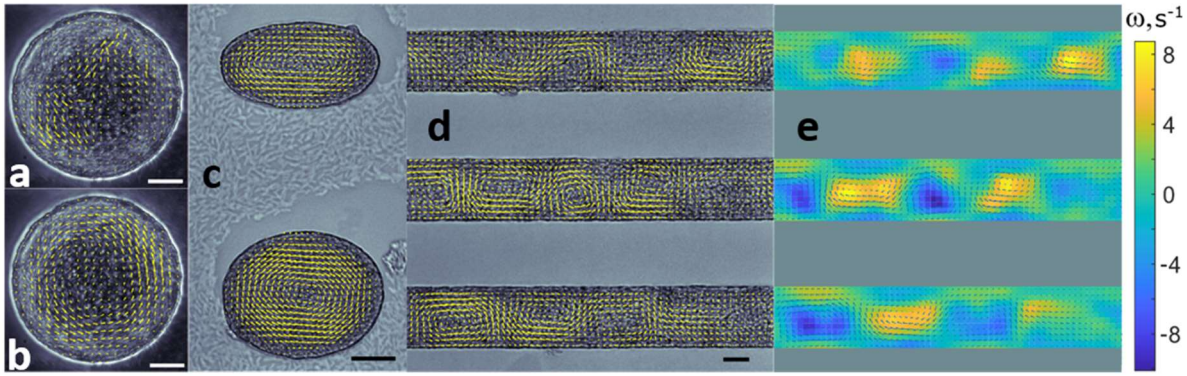

Figure 4. a) Agar well populated by swarming bacteria revealing the chaotic flow of bacterial active fluid. b) The flow field, $\vec{V}$, averaged over 1000 instantaneous fields reveals a mean spiral flow. c) Averaged fields in the wells of elliptical shape represent a stable elongated vortex. d) Averaged velocity field in a long rectangular groove is organized into a vortex lattice. e) Vorticity field, $\omega = \nabla \times \vec{V}$, calculated from panel d. Scale bar, 20 μm. Further details of this investigation will be published elsewhere.